Using Sum-Frequency Generation (SFG) to Probe Electric-Fields within Organic Field-Effect Transistors

Douglas J. C. Gomes[1], Silvia G. Motti[2] and Paulo B. Miranda[1]
[1]São Carlos Institute of Physics, University of São Paulo,
C.P. 369, São Carlos – SP, 13560-970, Brazil
[2]Center for Nano Science and Technology @PoliMi, Istituto Italiano di Tecnologia,
Via Pascoli 70/3, 20133 Milano, Italy

Keywords: Sum-Frequency Generation, Organic Transistors, Electric-Field Poling.

Abstract: Organic Field-Effect Transistors (OFETs) have attracted much research interest due to their potential for unique applications, such as flexible electronics. The operation of OFETs depends on the charge accumulation at the interface between an organic semiconductor and a dielectric material, induced by the voltage applied at the gate electrode. Direct measurements of the electric-field distribution in an operating device are useful for proposing and validating theoretical models for OFET operation. Here we propose using the second-order nonlinear optical process of Sum-Frequency Generation vibrational spectroscopy (SFG spectroscopy) to probe the presence of an electric-field in the dielectric layer of OFETs, in a non-invasive, non-destructive and remote fashion. The OFETs were fabricated with a dielectric layer consisting of poly(methyl-methacrylate) – PMMA, and an active layer based on poly(3-hexyl thiophene) – P3HT, and SFG spectra were acquired from the channel region of operating OFETs. It was observed the appearance of vibrational bands due to carbonyl groups (~ 1720 cm^{-1}) of the PMMA layer, whose $\chi^{(2)}$ were induced by the electric-field within the dielectric, similarly to a reversible poling of polymers. This phenomenon opens up the possibility of mapping the spatial charge distribution in the conducting channel using SFG microscopy in operating devices.

1 INTRODUCTION

Semiconductor devices based on organic materials, such as transistors or solar cells, have attracted much research interest due to their potential for unique applications, such as flexible and/or low-cost electronics. The operation of organic field-e□ect transistors (OFETs) depends on the modulation of charge accumulation at the interface between an organic semiconductor and a dielectric material, induced by the voltage applied at the gate electrode. The accumulated charge carriers form a conducting channel and are driven along this interface by application of an electric field parallel to the interface, between drain and source electrodes (Sze and Kwok, 2007). Although the basic physics of OFETs is well known, there is currently no single model that can explain its operation both in the linear regime and in saturation, after the pinch-off of the conduction channel (Stallinga and Gomes, 2006). Therefore, direct measurements of the electric field distribution in an operating device are useful for proposing and validating theoretical models.

Several methods have been used to probe the potential, field or charge distribution in operating OFETs, including Kelvin probe microscopy (Hallam et al., 2009), microwave conductivity microscopy (Babajanyan et al., 2011), charge modulation spectroscopy (Sciascia et al., 2011), Raman microscopy (Furukawa et al., 2012), and second-order nonlinear optical processes, such as second-harmonic generation (SHG) (Manaka et al., 2007a) and vibrational spectroscopy by sum-frequency generation (SFG) (Nakai et al., 2009). The optical methods have the advantage of being non-invasive, that is, they do not affect the charge distribution that is being probed. Among them, SHG and SFG are very versatile, since they allow probing the field distribution (Manaka et al., 2007a; Nakai et al., 2009) and dynamics (Manaka et al., 2007b) within the organic semiconductor. In this work, we further

Gomes, D., Motti, S. and Miranda, P.
Using Sum-Frequency Generation (SFG) to Probe Electric-Fields within Organic Field-Effect Transistors.
DOI: 10.5220/0005812801920196
In *Proceedings of the 4th International Conference on Photonics, Optics and Laser Technology (PHOTOPTICS 2016)*, pages 194-198
ISBN: 978-989-758-174-8

extend these methods by showing that SFG vibrational spectroscopy can be used to selectively probe the electric-field inside the dielectric layer of OFETs, which is directly related to the charge distribution in the OFET channel.

2 MATERIALS AND METHODS

2.1 Materials and Sample Preparation

The bottom-gate/top-electrode OFETs have been fabricated by sequential spin-coating of a dielectric layer consisting of poly(methyl-methacrylate) – PMMA, and an active layer based on poly(3-hexyl thiphene) – P3HT, using solutions made with orthogonal solvents. The PMMA layer was ~ 400 nm thick and was spin-coated from a methy-ethyl ketone solution, while the P3HT film was spin-coated over the PMMA film from a tetralin solution. The thickness of this P3HT film was only ~ 30 nm to minimize the absorption of the SFG light (wavelength ~ 480 nm) generated at the PMMA film, while exiting through the P3HT layer.

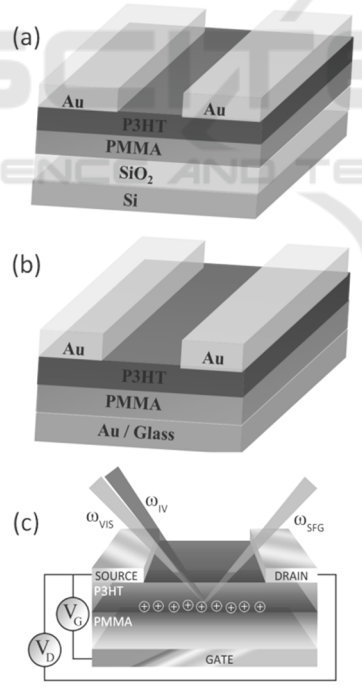

Figure 1: Scheme of the device structures: (a) Si/SiO_2/PMMA/P3HT/Au and (b) Glass/Au/PMMA/P3HT /Au. (c) Schematic view of the SFG spectroscopy experiment in the channel of the polarized device.

Two types of substrates were used: for the measurements of SFG spectra as a function of applied potential, we used n-doped Si wafers with a 300 nm thermal oxide layer as a gate electrode, while the temperature dependence was measured on a device fabricated on glass substrates, with the gate electrode produced by thermal evaporation of Au. The top electrodes were also evaporated Au films, with channel dimmensions L = 100 μm and W = 2 mm. The structure of the devices is shown in Figure 1, together with a scheme of the SFG experiment on a polarized device.

2.2 SFG Spectroscopy

The second-order nonlinear optical process of sum-frequency generation (SFG) is forbidden in media with inversion symmetry, so that it has been widely used to selectively probe the interfacial region between two materials, where the inversion symmetry is usually broken (Shen, 1996). In its conventional implementation for surface studies, two high intensity laser pulses (one usually in the visible and another tunable in the mid-infrared) is incident at the sample interface, and a sum-frequency beam is generated in the reflected direction due to the second-order polarization generated at the interface (see Equation (1)). The SFG intensity is proportional to the product of the input beam intensities and the square of the effective second-order susceptibility of the interface, $\chi_{eff}^{(2)}$, and it is measured with a photomultiplier, after spectral and spatial filtering. However, if a strong DC electric field E_0 is present in the bulk of a centrosymmetric material, it breaks the inversion symmetry and leads to a significant increase of the SFG signal. As shown in Equations (1) and (2), this increase of $\chi_{eff}^{(2)}$ has two contributions (Hayes, 2010): (i) a field-induced orientation of the dipoles in the material that leads to a non-vanishing $\chi^{(2)}(E_0)$, and (ii) a third-order contribution that mixes two laser fields E_{ω_1}, E_{ω_2} and the DC field E_0. They can be lumped together as an effective third-order contribution, which is proportional to the amplitude of the DC field, $\chi_{eff}^{(3)}E_0$. Therefore, if in the zero-field limit $\chi_{eff}^{(2)}$ is negligible, the SFG intensity is proportional to the square of the DC field in the material.

$$\vec{P}_{\omega_3} = \ddot{\chi}^{(1)} \cdot \vec{E} + \ddot{\chi}^{(2)} : \vec{E}_{\omega_2} \vec{E}_{\omega_1} + \ddot{\chi}^{(3)} : \vec{E}_{\omega_2} \vec{E}_{\omega_1} \vec{E}_0 + \cdots \quad (1)$$

$$\chi_{eff}^{(2)} = \chi^{(2)}(E_0) + \chi^{(3)}E_0 = \chi_{eff}^{(3)}E_0 \quad (2)$$

Our SFG experiments were performed with a commercial SFG spectrometer (Ekspla, Lithuania), which is based on a picosecond high energy Nd^{+3}:YAG laser (30 mJ, 20 Hz repetition rate, 1064 nm) and an OPG/OPA/DFG unit pumped by the third harmonic of the laser (355 nm), to generate tunable mid-IR beam from 1000 cm^{-1} to 4000 cm^{-1} with pulse energies at the sample attenuated to ~150 μJ. The visible beam pumping the sample was a portion (~10 μJ) of the second-harmonic of the laser (532 nm). The incidence angles were 51° and 60° for the mid-IR and visible beams, respectively. The SFG output beam direction was determined by phasematching along the surface plane, being ~ 59.2° for an IR frequency of 1700 cm^{-1}. In these conditions, the coherence length ($L_c = 1/\Delta k$) for the SFG process in the reflection direction was ~ 76 nm. This sets the maximum PMMA film thickness from which the SFG signal is coherently generated (being proportional to the square of the film thickness). However, since both types of OFET samples had reflective gate electrodes, we may also have collected simultaneously the SFG signal generated in the PMMA layer in the transmission direction, which was then reflected by the gate electrode. For the transmission geometry, the coherence length is much longer (~ 65 μm), so that in this case the whole PMMA film is contributing to the detected SFG signal.

3 RESULTS AND DISCUSSION

Figure 2 displays the electrical characteristics of the OFET on the Si substrate (Si/SiO_2/PMMA/ P3HT/Au). These output curves show a nice saturation and typical p-type OFET performance. However, it can be seen that they do not cross the origin, indicating that the gate leakage current is considerable, since the top contact pads had an area of ~16 mm^2, and the whole substrate is conductive.

Figure 3 shows the SFG spectra obtained in the channel region of the OFET on the Si substrate, for several gate voltages (keeping $V_D = 0$). It can be seen that upon polarizing the device, a vibrational resonance arises at ~1720 cm^{-1}, which is assigned to the C=O stretch of the PMMA monomer (its chemical structure is shown in the inset of Figure 3). We have checked this assignment by repeating the experiment on an OFET without the PMMA layer (only SiO_2 as dielectric), when the SFG peak disappeared. The solid line is a fit to Equation (3), which represents the superposition of a vibrational resonance at ω_0 with amplitude A and width Γ, plus a weak nonresonant background, $\chi_{NR}^{(2)}$.

$$I_{SFG}(\omega_{IR}) \propto \left|\chi_{eff}^{(2)}(\omega_{IR})\right|^2 = \left|\frac{A}{\omega_{IR} - \omega_0 + i\Gamma} + \chi_{NR}^{(2)}\right|^2 \quad (3)$$

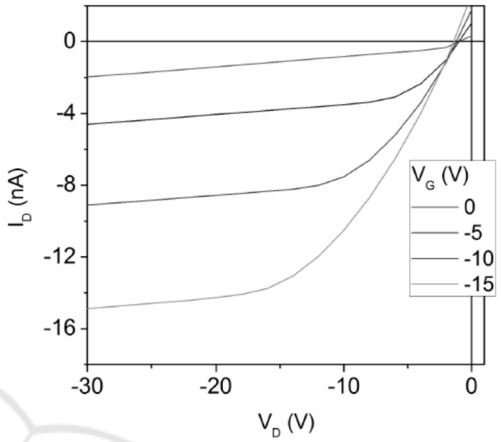

Figure 2: Output curves for the OFET with the structure: Si/SiO_2/PMMA/P3HT/Au.

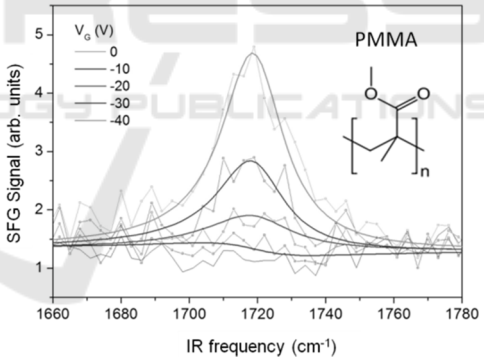

Figure 3: SFG spectra for the OFET on Si substrate, with several gate voltages, keeping $V_D = 0$. The solid lines are fits to Equation (3). The inset shows the chemical structure of the PMMA monomer.

From the fits, we can see that the amplitude A of the resonance increases nearly proportional to the applied gate voltage, as expected from Equation (2). Therefore, the amplitude of this peak can be used to probe the magnitude of the electric field within the organic dielectric layer (PMMA). The carriers accumulated at the semiconductor-dielectric interface could in principle give rise to an increase of the nonresonant contribution, $\chi_{NR}^{(2)}$, but this is not very significant, as can be seen from the fits and

from the SFG signal far off resonance (Figure 3). However, due to interference with the weak nonresonat background, we can see that the peak lineshape is a bit asymmetric. It is possible to exploit this interference to get not only the magnitude, but also the relative sign of the DC field within the PMMA layer. For that, we need a stronger $\chi_{NR}^{(2)}$, comparable to the resonant peak nonlinearity (A/Γ). With this purpose, we then fabricated the OFETs on glass substrates with Au films as gate electrodes. Gold has a high $\chi_{NR}^{(2)}$ at the wavelengths used, so that it provides a reference signal with which the resonant peak from PMMA interferes. Figure 4 shows the SFG spectra obtained for the device with the glass substrate (Glass/Au/PMMA/P3HT/Au), with both positive and negative gate voltages (and not polarized, as a reference). With V_G = 0, we detect only the nonresonant contribution from the Au electrode (gate). For negative gate voltages, we see that the vibrational peak from the C=O stretch of PMMA interferes destructively with the nonresonant background from Au, producing a dip in the spectrum. For positive voltages, the orientation of the C=O dipoles is inverted, changing the sign of the peak amplitude A and yielding a constructive interference with $\chi_{NR}^{(2)}$ and giving rise to a pronounced peak at the molecular resonance.

We could estimate the sensitivity of the method to detect electric fields in the dielectric layer (at least for these non-optimized conditions) by considering that the minimum detectable change in the spectra shown in Figure 3 occurs for V_G ~ - 10V. This corresponds to an E-field of about $2.5 \cdot 10^5$ V/cm.

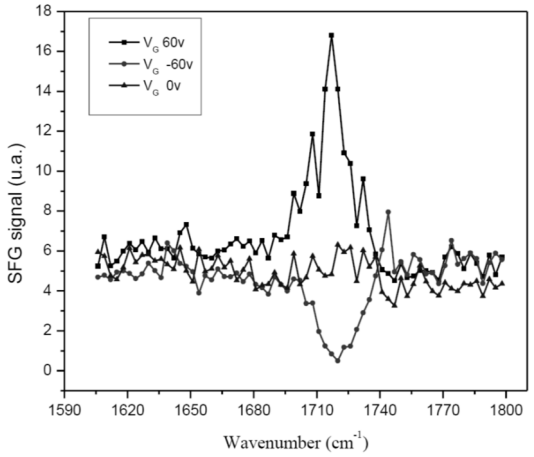

Figure 4: SFG spectra for the OFET with a Gold gate electrode (Glass/Au/PMMA/P3HT/Au), without and with both positive and negative gate voltages, keeping V_D = 0.

Finally, we tried to address the origin of the effective second-order nonlinearity that we have been measuring in our devices. Is $\chi_{eff}^{(2)}$ mostly due to the field-induced reorientation of the molecular dipoles (as in a fully reversible electric field poling of polymers (Bauer, 1996)), or is it a higher order $\chi_{eff}^{(3)} E_0$ contribution, that does not require any molecular reorientation in the solid polymer film and may happen in perfectly isotropic materials? In the first case, we should expect a strong temperature dependence of the resonant contribution $\chi_R^{(2)}$, as shown by Equation (4) (μ is the molecular dipole moment), provided that the DC field is not strong enough to reach dielectric saturation. If $\chi^{(3)}$ dominates, its temperature dependence should be rather weak, because it would not depend as strongly as $\chi^{(2)}$ on the average molecular orientation.

$$\chi_R^{(2)} \propto \frac{\mu E_{DC}}{k_B T} \tag{4}$$

Figure 5 shows the temperature dependence of the peak intensity of the spectrum in Figure 4, with V_G = +60 V. It can be seen that there is a significant decrease of the SFG intensity while heating the sample, which is reversible upon cooling, within the uncertainty of the measurement. The solid line represents a signal decrease as predicted by Equation (4). Therefore, these data support the conclusion that even for our samples, which are solid and should have a relatively low molecular mobility, the $\chi^{(2)}$ contribution due to DC field poling of the PMMA layer is the dominant contribution to the effective second-order nonlinearity. Any $\chi^{(3)}$ contribution appears to be negligible.

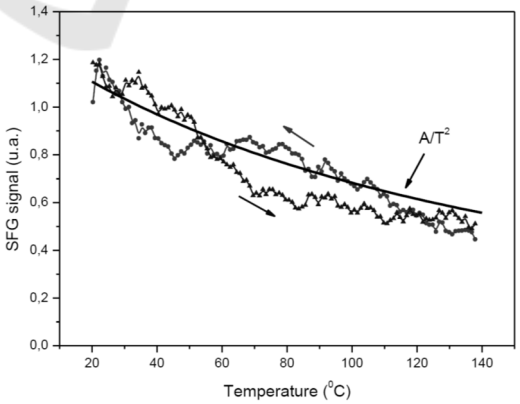

Figure 5: SFG signal for the OFET with a Gold gate electrode, biased with V_G = +60 V and V_D = 0, upon a heating and cooling cycle (heating/cooling rate ~ 2 °C/min). The solid line is the temperature dependence predicted by Equation (4).

4 CONCLUSIONS

Direct measurements of the electric-field distribution in an operating organic transistor are useful for proposing and validating theoretical models for their electrical behavior. Here we showed that Sum-Frequency Generation vibrational spectroscopy (SFG spectroscopy) is a valuable tool to probe the electric field within the (organic) dielectric layer of the transistor. The SFG spectra from polar groups of the dielectric (PMMA) show a marked resonance, whose amplitude is proportional to the applied gate voltage, which in turn is proportional to the field within the dielectric, when $V_D = 0$. Using the interference of this resonant contribution with a large nonresonant background from the gate electrode, it is possible to determine not only the relative magnitude of the field within the dielectric, but also its sign. We further demonstrated that even for solid samples, where the dipoles are less mobile than in the case of organic molecules in solution, the $\chi^{(2)}$ contribution due to DC field reorientation of the dielectric layer is the dominant contribution to the effective second-order nonlinearity, and any $\chi^{(3)}$ contribution appears to be negligible. This phenomenon allows probing the electric field in the dielectric, which is directly related to the charge distribution in the OFET channel, and opens up the possibility of mapping the spatial field distribution in the conducting channel by SFG microscopy of OFETs (Nakai et al., 2009).

ACKNOWLEDGEMENTS

DJCG gratefully acknowledges a PhD scholarship from FAPESP and SGM thanks CAPES for a MSc scholarship. This work has been supported by the Brazilian agencies FAPESP and CNPq.

REFERENCES

Babajanyan, A., Melikyan, H., Kim, J., Lee, K., Iwamoto, M., Friedman, B., 2011. Direct imaging of conductivity in pentacene field-effect transistors by a near-field scanning microwave microprobe. *Org. Electron.* 12, 263–268.

Bauer, S., 1996. Poled polymers for sensors and photonic applications. *J. Appl. Phys.* 80, 5531–5558.

Furukawa, Y., Seto, K., Nakajima, K., Itoh, Y., Eguchi, J., Sugiyama, T., Fujimura, H., 2012. Infrared and Raman spectroscopy of organic thin films used for electronic devices. *Vibr. Spectrosc.* 60, 5–9.

Hallam, T., Lee, M., Zhao, N., Nandhakumar, I., Kemerink, M., Heeney, M., McCulloch, I., Sirringhaus,H., 2009. Local charge trapping in conjugated polymers resolved by scanning Kelvin probe microscopy. *Phys. Rev. Lett.* 103, 256803.

Hayes, P. L., Malin, J. N., Jordan, D. S., Geiger F. M., 2010. Get charged up: Nonlinear optical voltammetry for quantifying the thermodynamics and electrostatics of metal cations at aqueous/oxide interfaces. *Chem. Phys. Lett.* 499, 183–192.

Manaka, T., Nakao, M., Yamada, D., Lim E., Iwamoto M., 2007 a. Optical second harmonic generation imaging for visualizing in-plane electric field distribution. *Optics Express* 15, 15964-15971.

Manaka, T., Lim E., Tamura, R., Iwamoto M., 2007 b. Direct imaging of carrier motion in organic transistors by optical second harmonic generation. *Nat. Photonics* 1, 581-584.

Nakai, I. F. *et al.*, 2009. Molecular structure and carrier distributions at semiconductor/dielectric interfaces in organic field-effect transistors studied with sum-frequency generation microscopy. *Appl. Phys. Lett.* 95, 243304.

Sciascia, C. *et al.*, 2011. Sub-micrometer charge modulation microscopy of a high mobility polymeric n-channel field-effect transistor. *Adv. Mater*. 23, 5086–5090.

Shen, Y. R., 1996. A few selected applications of surface nonlinear optical spectroscopy. *Proc. Natl. Acad. Sci. USA* 93, 12104.

Stallinga, P., Gomes, H., 2006. Modeling electrical characteristics of thin-film field-effect transistors I: trap-free materials. *Synth. Met*. 156, 1305–1315.

Sze, S. M., Kwok, K. Ng., 2007. *Physics of Semiconductor Devices*, Wiley, New Jersey.